JOURNAL OF ZOOLOGICAL SYSTEMATICS AND EVOLUTIONARY RESEARCH

Accepted on 11 January 2013
J Zoolog Syst Evol Res doi: 10.1111/jzs.12054

[1]*Research Group Marine Biology, Biology Department, Ghent University, Ghent;* [2]*Center for Molecular Phylogenetics and Evolution (CeMoFe), Ghent University, Ghent Belgium;* [3]*Department of Invertebrate Zoology, Faculty of Biology, Lomonosov's Moscow State University, Moscow;* [4]*P.P. Shirshov Institute of Oceanology, Russian Academy of Sciences, Moscow, Russia*

The *Halomonhystera disjuncta* population is homogeneous across the Håkon Mosby mud volcano (Barents Sea) but is genetically differentiated from its shallow-water relatives

Van Campenhout Jelle[1,2], Derycke Sofie[1,2], Tchesunov Alexei[3], Portnova Daria[4] and Vanreusel Ann[1]

Abstract

The deep sea has a high biodiversity and a characteristic bathyal fauna. Earlier evidence suggested that at least some shallow-water species invaded the ecosystem followed by radiation leading to endemic deep-sea lineages with a genetic and/or morphological similarity to their shallow-water counterparts. The nematode *Halomonhystera disjuncta* has been reported from shallow-water habitats and the deep sea [Håkon Mosby mud volcano (HMMV)], but the morphological features and the phylogenetic relationships between deep-sea and shallow-water representatives remain largely unknown. Furthermore, nothing is known about the genetic structure of the *H. disjuncta* population within the HMMV. This study is the first integrative approach in which the morphological and phylogenetic relationships between a deep-sea and shallow-water free-living nematode species are investigated. To elucidate the phylogenetic relationships, we analysed the mitochondrial gene *Cytochrome oxidase c subunit I* (*COI*) and three nuclear ribosomal genes (*Internal Transcribed Spacer region*, *18S* and the *D2D3* region of *28S*). Our results show that deep-sea nematodes comprise an endemic lineage compared to the shallow-water representatives with different morphometric features. *COI* genetic divergence between the deep-sea and shallow-water specimens ranges between 19.1% and 25.2%. Taking these findings into account, we conclude that the deep-sea form is a new species. AMOVA revealed no genetic structure across the HMMV, suggesting that nematodes are able to disperse efficiently in the mud volcano.

Key words: Deep sea – Håkon Mosby mud volcano – *Halomonhystera* – population genetics – cryptic species

Introduction

The deep sea represents the largest ecosystem on earth and supports a high species diversity (Hessler and Sanders 1967), which, however, remains to date largely uninvestigated (Levin and Sibuet 2012). Identifying and understanding this hidden component of biodiversity is one of the major challenges for deep-sea biologists. Fossil evidence (Hessler and Thistle 1975; Jablonski and Bottjer 1988; Sepkoski 1991) suggests that shallow-water echinoderms and isopods have dispersed to the deep sea followed by adaptive radiation and retreat from shallow-water habitats resulting in strictly deep-sea 'endemic' lineages. In addition, evidence from isopods shows that deep-sea populations are a mixture of old and recently dispersed taxa as a result of multiple independent colonizations of the deep sea (Wilson 1998; Brandt et al. 2007). The initial step in speciation between intertidal and deep-sea populations is a geographical separation that interrupts gene flow between both populations. This separation can then be followed by ecological adaptations to local environmental conditions and/or the rapid evolution of genes linked to mate recognition (Taylor and Hellberg 2005). Morphologically and/or genetically closely related representatives from deep-sea and shallow-water habitats have been reported for a variety of invertebrates, ranging from Hydrozoa (Moura et al. 2012), Foraminifera (Pawlowski et al. 2007), Polychaeta (Nygren et al. 2010), Gastrotricha (Kieneke et al. 2012), Porifera (Reveillaud et al. 2010) and Nematoda (Bik et al. 2010).

Nematodes are the most abundant and arguably the most diverse metazoan phylum in terms of species richness in the animal kingdom (Lambshead 2004). Many nematode species have a worldwide distribution, despite an endobenthic life style, a lack of pelagic larvae and supposedly limited dispersal capacity (Palmer 1988). However, transoceanic distribution of *Litoditis marina* suggests that effective long-distance dispersal can occur (Derycke et al. 2008b). The widespread distribution of species may further be complicated by the presence of cryptic species, that is morphologically similar but genetically distinct species. The occurrence of cryptic species can transform what was previously thought to be a generalist species with widespread distribution into several specialist species with more restricted distributions. Cryptic species have been reported in marine nematodes belonging to different orders (Derycke et al. 2005, 2007a, 2008a, 2010a), illustrating that knowledge of their presence is important for correctly interpreting biodiversity patterns in different habitats.

Interestingly, most marine nematode genera and also several species have been identified as occurring in shallow-water environments as well as in deep-sea habitats (Heip et al. 1985; Muthumbi et al. 2004; Fonseca et al. 2007; Van Gaever et al. 2009b; Vanreusel et al. 2010). Repeated and recent interchanges between the deep-sea and intertidal zone have been observed (Bik et al. 2010), supporting the idea that habitat transitions are frequent and common among nematodes (Holterman et al. 2008). In contrast, the evolutionary relationships and connectivity patterns between deep-sea and shallow-water populations of a single species remain unstudied.

The genus *Halomonhystera* belongs to the Monhysteridae, a common family of nematodes often highly represented in both shallow and deep-water environments. Andrássy (1981) initially included *Monhystera disjuncta* with related species in the genus *Geomonhystera* (Andrássy, 1981). Later, Andrássy (2006) divided the genus *Geomonhystera* into two morphologically and ecologically distinct groups and placed *G. disjuncta* and related marine and brackish species into the newly created genus *Halomonhystera* (Andrássy, 2006). Species from this genus also inhabit sulphidic environments in the deep sea such as vents and seeps (Van Gaever et al. 2006; Zekely et al. 2006; Copley et al. 2007; Gollner et al. 2007). In this study, we focus on the free-

Corresponding author: Van Campenhout Jelle (jelle.vancampenhout@ugent.be)
Contributing authors: Derycke Sofie (s.derycke@ugent.be), Tchesunov Alexei (avtchesunov@ya.ru), Portnova Daria (daria.portnova@gmail.com), Vanreusel Ann (Ann.vanreusel@ugent.be)

living marine bacterivorous species *Halomonhystera disjuncta* known from shallow and deep-sea environments. *Halomonhystera disjuncta* can be distinguished from the other six marine species from this genus by differences in body size, position of the vulva, shape and length of the tail, mode of reproduction (oviparity or viviparity), and shape and number of eggs (Stekhoven et al. 1931; Hopper 1969). *Halomonhystera disjuncta* is further known for its high tolerance to temperature changes and high heavy metal concentrations (Vranken et al. 1985, 1988b, 1989). In addition, it is a fast colonizer in shallow waters, successfully exploiting organically enriched substrata such as sediments from estuarine mudflats (Heip et al. 1985) or decomposing algal thalli (Derycke et al. 2007b). Both features could explain the occurrence of *H. disjuncta* in different environments (deep sea and shallow water). In addition, it is abundant on decomposing macroalgae which can be transported over large distances and could explain in part the occurrence of *H. disjuncta* over a large geographical area. *Halomonhystera disjuncta* has been reported from different geographical areas including Western Canada (Trotter and Webster 1983), the White Sea in northern Russia (Mokievsky et al. 2005), the North Sea South of Norway (Vranken et al. 1988a) and along the coast of Belgium and the south-western part of the Netherlands (Derycke et al. 2007a). A recent study showed that *H. disjuncta* from the southern North Sea actually consists of five cryptic species (Derycke et al. 2007a) with subtle morphometric differences (Fonseca et al. 2008). Up to three of these species co-occurred in a single location, and genetic structuring was low when populations were compared within an estuary (Derycke et al. 2007a). Interestingly, *H. disjuncta* has also been reported in unusually high densities (11 000 ind. per 10 cm^{-2}) at the Håkon Mosby mud volcano (HMMV) at a depth of 1280 m in the Barents Sea (Van Gaever et al. 2006) and occurred in high densities at the Nyegga pockmarks (Portnova et al. 2010). However, it remains unclear how this deep-sea *H. disjuncta* population is related to the shallow-water species complex. Such information is, however, critical in assessing whether the same species can occur in both shallow and deep-sea environments.

We investigated nematode population structure at the HMMV. The HMMV is an active mud-expelling and methane-venting volcano located on the South West Barents Sea slope (72°00.25′ N/14°43.50′E) discovered in 1999 (Vogt et al. 1999). The cake-shaped caldera is 1 km in diameter and has an 8–10 m rise from the foot. The central zone of the caldera is about 200 m in diameter and characterized by strongly reduced conditions; methane concentration in the surface sediment layer and in the water just above the sediment reaches here 12.5 and 6 ml l^{-1}, respectively (Sauter et al. 2006). The HMMV incorporates several habitats that differ in microbial and megafaunal community composition (Niemann et al. 2006) such as (1) the active central zone with a high mud flow, (2) the zone covered with *Beggiatoa* mats and with highly sulphidic sediments (Pimenov et al. 2000; Lichtschlag et al. 2010) and (3) the *Siboglinidae* fields (Vogt et al. 1997; Gebruk et al. 2003; Losekann et al. 2008). *Halomonhystera disjuncta* thrives with unusually high densities in the whitish bacterial *Beggiatoa* mats of the HMMV that cover the sediment around the central zone and that form an important food source for *H. disjuncta* (Van Gaever et al. 2009a). Observations in 2009 and 2010 revealed that just north of the centre, new *Beggiatoa* mats colonized the previously bare sediment which was then followed by a colonization of nematodes. The source origin of the nematodes in the newly colonized area and the connectivity of populations within the HMMV are, however, unknown.

Here, we investigated how the *H. disjuncta* specimens from the sulphidic bacterial mat-covered zone of the HMMV are related to the intertidal cryptic species. For this, we amplified one mitochondrial and three nuclear genes to infer species identity and phylogenetic relationships. The phylogenetic species concept (Adams 1998) was used to delineate species. Subsequently, a detailed morphological analysis was conducted to investigate whether morphological differences accompanied the molecular phylogenetic clades. Finally, the population genetic structure of *H. disjuncta* within the HMMV was investigated using *Cytochrome oxidase c subunit* I (*COI*) to reveal colonization patterns and connectivity in these remote and highly reduced deep-sea sediments.

Materials and Methods

Study area

We investigated specimens identified earlier as *H. disjuncta* (Van Gaever et al. 2006; Portnova 2009) from the active methane-seeping Håkon Mosby mud volcano (HMMV, Fig. 1), situated west of the Barents Sea (72.1°N 14.73°E) at an average water depth of 1280 m. We studied three locations within the HMMV characterized by thiotrophic bacterial mat cover, the north (N, 72°0.29′N 14°43.61′E, Station MSM16-2_841-1), south-east (SE, 72°0.17′N, 14°43.88′E, Station MSM16-2_802-1) and south-west (SW, 72°0.14′N, 14°43.21′E, Station MSM16-2_857-1). The distance between N-SE, SE-SW and SW-N is 270, 387 and 360 m, respectively.

Sampling strategy

Sediment samples were collected in the north (N), south-east (SE) and south-west (SW) of the HMMV (Fig. 1) during the Maria S. Merian cruise 2010 (MSM 16/2). Utilizing a TV-guided multicorer (TV-muc), we were able to aim for bacterial mats, the preferred habitat of *H. disjuncta*. Samples for both morphological and molecular purposes were immediately sliced from 0 to 10 cm with a one cm interval. Samples for molecular analysis were frozen in liquid nitrogen onboard and stored at −80°C. Other samples were fixed in 4% buffered formaldehyde. Three replicates were sampled in each region and processed according to the same protocol.

Sequence data

Halomonhystera disjuncta has very high densities in the top centimetres of the HMMV bacterial mat sediments (Van Gaever et al. 2006). Therefore, DNA was extracted (following the procedure of Derycke et al. 2005) from 155 specimens from the first centimetre of the three different geographical locations in the HMMV (51 specimens from the South East, 50 specimens from the North and 54 specimens from the South West). After DNA preparation, we amplified 425 base pairs (bp) of the mitochondrial *Cytochrome oxidase c subunit I* (*COI*) gene with the primers JB2 (5′-ATGTTTT GATTTTACCWGCWTTYGGTGT-3′) and JB5GED (5′-AGCACCTAA ACTTAAAACATARTGRAARTG-3′) from Derycke et al. (2007a) yielding sequence fragments for two individuals from each of the three locations (Table 1). Based on these sequences, new primers were developed to increase the amount of successful amplifications: JB2_HD_HMMV (5′-TG AGGCATTCTATTATATATATGTCGG-3′; 30 bp downstream of JB2) and JB5_HD_HMMV (5′-AGCAACAACATAGTAAGTATCGTG-3′; 30 bp upstream of JB5GED). Using these primers, we amplified a 365 bp region of the *COI* gene of an additional 45, 46 and 51 nematodes from the SE, N and SW, respectively, of the HMMV. After removal of the primers and checking for insertions and deletions, we ended up with a fragment of 314 bp. Haplotypes were inferred from good sequence spectra, that is without any ambiguous nucleotide positions, from 25, 32 and 33 nematodes from the SE, N and SW, respectively (accession numbers: HF572956, HF572957, HF572959, HF572960 and HF572966). Sequences showing ambiguous positions were removed from the data set. Standard PCR amplifications were conducted in 25 µl volumes for 40 cycles, each consisting of a 30 s denaturation at 94°C, 30 s annealing at 54°C and 30 s extension at 72°C, with an initial denaturation step of 5 min at 94°C and a final exten-

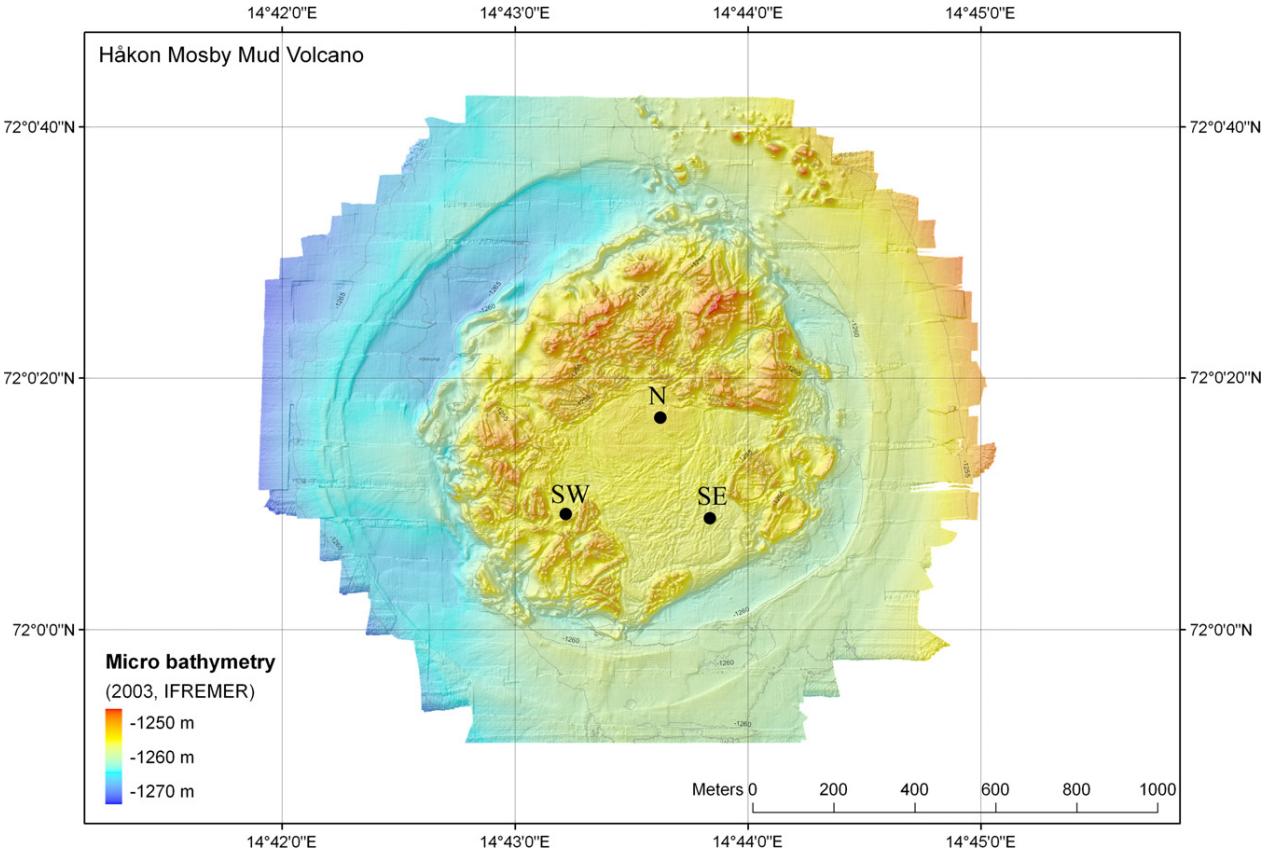

Fig. 1. Sampling points on the bathymetrical map of the Håkon Mosby mud volcano. We have sampled the North (N, 72°0.29′N 14°43.61′E, Station MSM16-2_841-1), South East (SE, 72°0.17′N, 14°43.88′E, Station MSM16-2_802-1) and South West (SW, 72°0.14′N, 14°43.21′E, Station MSM16-2_857-1). (Adapted from Foucher et al. 2010).

Table 1. Sequence identity and accession numbers for each specimen used for amplification of three nuclear markers (*18S rDNA* gene, *D2D3* region of *28S rDNA* and *Internal Transcribed Spacer region* (*ITS*) and one mitochondrial marker [*Cytochrome oxidase c subunit I* (*COI*)]. The *18S*, *ITS* and *D2D3* nuclear marker sequences were amplified with respective primer combinations: G18S4 – 18P, Vrain2F – Vrain2R and D2/F1 – D3b. The *COI* gene fragment of six individuals (*) was amplified with JB2 – JB5GED. All other *COI* sequence markers were amplified with JB2_HD_HMMV – JB5_HD_HMMV. Specimen codes consist of the location within the HMMV, South East (SE), North (N) and South West (SW) followed by the number of the specimen.

Marker sequence	Haplotypes	Accession numbers	South East (SE)	North (N)	South West (SW)
18S	–	HF572952	SE1-5	N9, N10, N18, N19, N21	SW5, SW10, SW13, SW14, SW18
ITS	–	HF572967	SE1-6, SE8-11	N9, N10, N18, N19, N21, N24, N25, N28, N29, N30	SW5, SW10, SW13, SW14, SW18, SW21, SW22, SW25, SW26, SW29
D2D3	–	HF572953	SE1-5	N9, N10, N18, N19, N21	SW5, SW10, SW13, SW14, SW18
COI	Haplotype A	HF572956	SE11	–	SW5*
	Haplotype B	HF572957	SE3, SE14, SE26	–	SW16, SW22
	Haplotype C	HF572966	SE2, SE4, SE5, SE8, SE9, SE19, SE21, SE29, SE31*, SE33*, SE35, SE39, SE40, SE48	N9*, N10*, N16, N18, N19, N25, N26, N27, N31, N32, N36, N39, N43, N44, N45, N47, N48, N49, N50	SW8, SW10*, SW18, SW21, SW24, SW25, SW26, SW29, SW35, SW36, SW39, SW41, SW43, SW46, SW49, SW50, SW53, SW54,
	Haplotype D	HF572959	SE7, SE24, SE25, SE34, SE37	N2, N6, N11, N12, N15, N21, N23, N24, N30, N42	SW9, SW11, SW14, SW17, SW30, SW33, SW37, SW47
	Haplotype E	HF572960	SE6,SE43	N28, N29, N38	SW13, SW40, SW45, SW55

sion step of 10 min at 72°C. We loaded 4 µl of each PCR product onto a 1% agarose gel to determine the size of the amplified product.

In addition, ca. 1700 bp of the ribosomal *18S* gene were amplified with primers G18S4 (5′-GCTTGTCTCAAAGATTAAGCC-3′) and 18P (5′-TGATCCWMCRGCAGGTTCAC-3′) for five nematodes from each of the three sampling locations on the HMMV (Table 1). PCR conditions were the same to those for amplification of the *COI* fragment except for the extension step in which the time was increased to 120 s.

The Internal Transcribed Spacer region (*ITS*) was amplified (accession number: HF572967) using primers Vrain2F (5′-CTTTGTACACACCG CCCGTCGCT-3′) and Vrain2R (5′-TTTCACTCGCCGTTACTAAGGGA ATC-3′). PCR conditions were the same to those described above except for the extension step in which the time was set at 60 s. For *ITS*, we were able to retrieve sequences of ca. 900 bp for 10 individuals from each of the three sampling locations (Table 1).

A third nuclear fragment, the *D2D3* region (ca. 300 bp) of the ribosomal *28S* gene, was amplified using D2/F1 (5′-TTCGACCCGTCTTG AAACACG-3′) and D3b (5′-TCCTCGGAAGGAACCAGCTACTA-3′) and yielded sequence fragments for five individuals from each of the three sampling regions (Table 1, accession number: HF572953). PCR conditions were the same to those previously described, only the extension time was set at 45 s.

All gene fragments were Sanger-sequenced by Macrogen Inc. (http://www.macrogen.com). *COI*, *ITS* and *D2D3* gene fragments were bidirectionally sequenced with the above-described primers. The 5′ region of the *18S rDNA* gene was sequenced with the primers G18S4, 9Fx (5′-AAGTCTGGTGCCAGCAGCCGC-3′), 4R (5′-GTATCTGATCGCCKTC GAWC-3′) and 23R (TCTCGCTCGTTATCGGAAT-3′) for five individuals from each of the three locations because the *18S* sequences of GD1-5 were limited to the first 700–900 bp. In addition, six individuals in total (two from each location) were sequenced completely with additional primers 18P, 4F (5′-CAAGGACGAWAGTTWGAGG-3′) and 23F (5′-ATTCCGATAACGAGCGAGA-3′) to obtain a 1726-bp-long sequence for GenBank submission (accession number: HF572952).

Morphometric data

Formaldehyde-fixed samples from the first centimetre were washed over a 32-μm mesh sieve, and nematodes were extracted by density-gradient centrifugation, using Ludox (a colloidal silica polymer; specific gravity 1.18) as a flotation medium (Heip et al. 1985). The extracted nematodes were stained with rose bengal in a 4% buffered formaldehyde solution. Nematodes were sorted using a binocular microscope and were placed into embryo dishes containing Seinhorst solution (70 parts of distilled water, 29 parts 95% ethanol and one part of glycerine) (Seinhorst 1959). Specimens were then mounted into permanent glycerine slides with a paraffin ring.

Using a Leica MM AF NX microscope, we measured 12 different parameters: length (L), pharynx length (PL), amphid-anterior distance (A-A), head diameter (Hdia), anus-anterior length (AL), maximum body width (W), vulva-anus distance (V-A) or spicule length (SL), anal body diameter (ABD), tail length (TL, from anus till the end of the tail), progaster diameter (PD) and the progaster corresponding body diameter (PCBD). In addition to *H. disjuncta* from the South East part of the HMMV (HD-HMMV) location, we also measured these parameters in specimens belonging to the five cryptic species from the intertidal zone. These specimens were retrieved from a previous study (Derycke et al. 2007a; Fonseca et al. 2008) and have been preserved and transferred into glycerine slides according to the same protocols.

Data processing

Sequence data

Contigs of individual fragments (*18S*, *ITS*, *D2D3* and *COI*) were created using SeqMan (Lasergene®; DNASTAR). Forward and reverse primers were removed, and sequences were blasted against known sequences of *H. disjuncta* and GenBank. The newly retrieved sequences were analysed together with published sequences of the five intertidal cryptic species (Derycke et al. 2007a). Finally, a *Diplolaimelloides meyli* (AM748759.1) sequence was added to the *COI* alignment. All nuclear phylogenetic analyses were performed in the absence of an outgroup. Consequently, trees were mid-point rooted.

All four data sets (*18S*, *ITS*, *D2D3* and *COI*) were aligned in CLUSTALX v1.74 (Thompson et al. 1997) using default alignment parameters (gap opening/gap extension costs of 15/6.66). The alignment ends were cropped to remove parts where only some sequences had data. The aligned sequences were used for further phylogenetic analysis in PAUP*4.0 beta 10 (Swofford 1998). Prior to phylogenetic tree construction, MODELTEST 3.7 (Posada and Crandall 1998) using the Akaike information criterion (Posada and Buckley 2004) was used to determine the evolutionary model for constructing neighbour joining (NJ) and maximum likelihood (ML) phylogenetic trees. The models selected for *18S*, *ITS*, *D2D3* and *COI* were GTR + I (Tavaré 1986), GTR + G, HKY + I (Hasegawa et al. 1985) and TrN + I + G (Tamura and Nei 1993), respectively. The best model for Bayesian analysis (BA) was determined with MRMODELTEST 2.2 (Nylander 2004) using the Akaike information criterion. The selected models for BA were GTR + I, GTR + G, HKY + I and HKY + I + G for *18S*, *ITS*, *D2D3* and *COI,* respectively.

Maximum parsimony (MP), NJ and ML trees were calculated in PAUP using heuristic searches and a tree-bisection-reconnection branch swapping algorithm (10 000 rearrangements) and a random stepwise addition of sequences in 100 replicate trials. One tree was held at each step. Bootstrap values for MP, NJ and ML were inferred from 1000, 1000 and 100 replicates, respectively. In addition, a BA was performed in MRBAYES v3.2 (Ronquist et al. 2012). Four independent Markov chains were run for 500 000 generations, with a tree saved every 100th generation. The first 1000 trees were discarded as burn-in.

We subsequently performed an incongruence length difference (ILD) test (Mickevich and Farris 1981) in PAUP, to investigate whether the different nuclear gene fragments could be combined in one analysis. Because we lacked *18S* sequences for several GD nematodes for which we had both *ITS* and *D2D3* sequences, we did not add the *18S* sequence to the concatenated data set. Consequently, the *18S* gene marker was analysed separately. The combined data set (*ITS* + *D2D3*) was used to construct MP, NJ, ML and BA trees, based on the GRT + G model, calculated as described above. Trees were mid-point rooted.

Pairwise uncorrected p-distances between HD-HMMV and GD1-5 were computed using MEGA 5.05 (Tamura et al. 2011). Insertions and deletions were pairwise deleted.

Morphometric data

The clades recovered in the phylogenetic analyses were used to group specimens for further morphometric analyses. All statistical analyses were performed using the STATISTICA 7.0 software package (StatSoft 2001). The morphological data were thoroughly checked for outliers, but no measurements had to be removed. To minimize effects of body length differences between nematodes, the continuous variables were divided by the total body length of the nematode followed by a log transformation. Afterwards, each parameter was tested for homogeneity of variances/covariances (Levene's test) and correlations between means and variances (visual assessment). The maximum body width (*W*) was removed from the data set because of a significant Levene's test ($p = 0.000002$). We also performed a pairwise correlation between the length (*L*) normalized morphometric parameters. The anus-AL was correlated ($R > 0.90$) with both pharynx (PL) and TL and was therefore removed prior to further analysis.

Univariate analysis of variance (ANOVA) was performed, in case of homogeneity of variances (Levene's test) and normal distribution (Shapiro–Wilk's normality test), to test whether the different species showed significant differences in morphometric measurements. In cases where homogeneity of variances was violated, even after log transformation of the raw data, a nonparametric test was used (Kruskal–Wallis). Both female and male data sets (without anus-AL and maximum body width due to violation of homogeneity of variances) were subjected to a backward stepwise discriminant function analysis (DFA; Klecka 1980; Garson 2008). DFA finds linear combinations of variables (roots) that maximize differences among *a priori* defined groups (in this case species). The classification success rate was evaluated based on the percentage of individuals correctly classified in the original sample.

Population genetic structure

The *COI* sequences obtained from 90 specimens from three locations in the HMMV (25, 32, 33 specimens from the SE, N and SW respectively) were used to assess the genetic diversity and structure in this highly specialized deep-sea habitat. Nucleotide (π) and haplotype diversity (h) and their standard deviation were calculated with ARLEQUIN v.3.0 (Excoffier et al. 2005). Analysis of molecular variance (AMOVA) applying Tamura–Nei distances (Tamura and Nei 1993) was used to investigate the percentage of variation within and between locations. Significance levels were determined with 1000 permutations. Population pairwise Φ_{ST} values were calculated using Tamura–Nei distances. A minimum spanning network was created using TCS1.21 (Clement et al. 2000) and was adapted to incorporate the haplotype frequencies using Excel and PowerPoint.

Results

Sequence data: phylogenetic analysis of *COI* from HMMV and shallow-water specimens

A total of 314 bp of the *COI* gene were screened from 25, 32 and 33 HD-HMMV individuals from the South East, the North and the South West, respectively. In total, four variable sites were observed that resulted in five different haplotypes (A–E). After combining the five observed HD-HMMV *COI* haplotypes with the published sequences of the five intertidal cryptic species GD1–GD5 (Derycke et al. 2007a), the alignment (Supporting information) used for phylogenetic analysis consisted of 49 sequences and was 343 bp long. At the 5′ and 3′ end, HD-HMMV sequences were respectively 29 bp shorter and 32 bp longer compared to GD1-5 sequences. The alignment contained 153 variable sites, of which 124 were parsimony informative. Not all substitutions were synonymous, and the amino acid alignment (114 amino acids long) yielded 32 variable sites. No start/stop codons and insertions/deletions (indels) were observed. The alignment was subjected to four different methods for phylogenetic tree construction: MP, NJ, ML and BA. The MP consensus tree was inferred from 35 most parsimonious trees of length 384. The consistency index (CI) was 0.6328, and the retention index (RI) was 0.9250. The optimal NJ phylogenetic tree (tree length = 395) had a CI of 0.6152 and a RI of 0.9191. Negative ln likelihood values for ML and BA phylogenetic trees were 2094.29 and 2163.19, respectively.

All methods used (MP, NJ, ML and BA) showed six distinct clades (Fig. 2, Figures S1–S3). Even though GD1 and GD4 were always observed close together (bootstrap values: 83–100), as well as GD2 and GD5 (bootstrap values: 73–100), the clustering was not highly supported in the NJ and MP analysis. Furthermore, the position of GD3 and HD-HMMV remained ambiguous. Based on our *COI* data, HD-HMMV is clearly differentiated from individual intertidal clades (GD1-5) with divergences ranging between 19.1% and 25.2%. The presence of GD4 haplotype G16 resulted in a maximum interspecific uncorrected p-distance of 10.9% within the GD4 lineages. Leaving haplotype G16 out of the data set revealed that divergence ranges were much lower within lineages (0.3–2.9%) than between lineages (13.3–25.7%, Table 2).

Sequence data: phylogenetic analysis of *18S*, *D2D3* and *ITS* from HMMV and shallow-water specimens

The alignments used for phylogenetic tree construction of the three nuclear sequences (*18S*, *D2D3* and *ITS*) had a length of 760, 299 and 909 bp, respectively. The *18S* alignment contained 175 variable sites, of which 168 were parsimony informative. Seven indel positions were observed ranging from 1 to 2 bp in

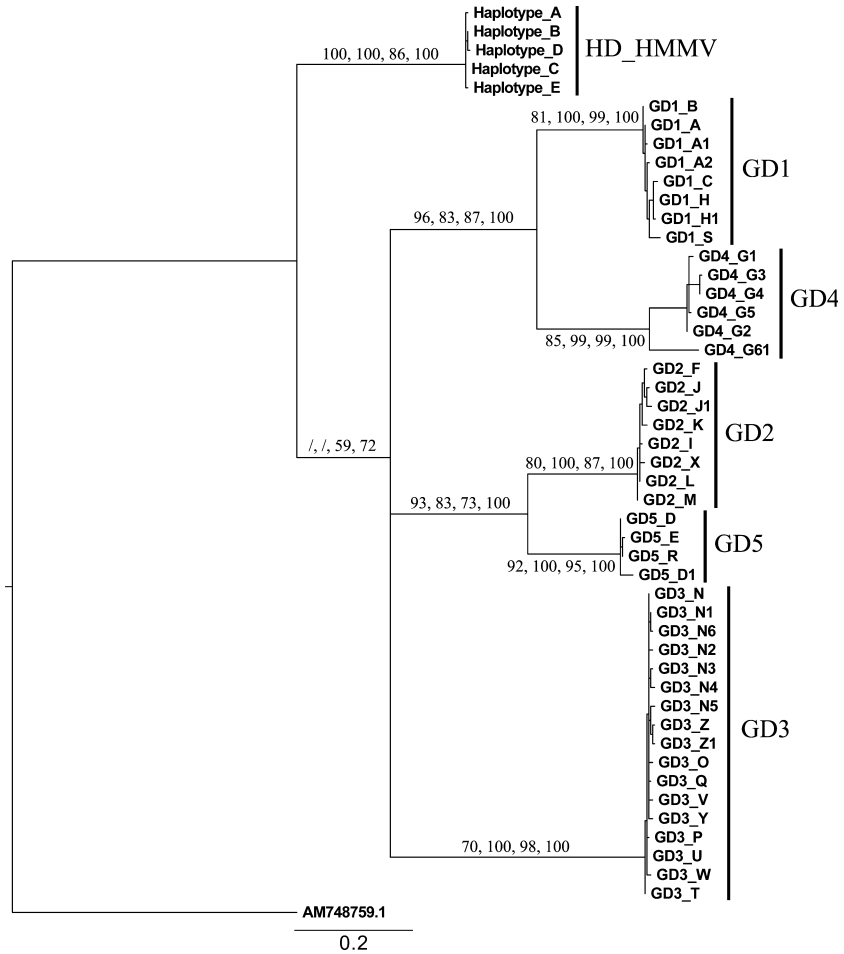

Fig. 2. Maximum likelihood (ML) tree of a heuristic analysis of the mitochondrial *Cytochrome oxidase c subunit I* (*COI*) gene of shallow-water [*Halomonhystera disjuncta* 1-5 (GD1-5)] and deep-sea (HD-HMMV) nematodes. Bootstrap values correspond to ML, maximum parsimony, neighbour joining and Bayesian analysis. A slash indicates the absence of a branch in the respective analysis. The outgroup AM748759.1 is *Diplolaimelloides meyli*.

Table 2. Intra- (diagonally) and interspecific minimum-maximum of uncorrected p-distances (%) between *Cytochrome oxidase c subunit I* (*COI*) sequences of five intertidal *Halomonhystera disjuncta* species (GD1-5) and *H. disjuncta* nematodes from the Håkon Mosby mud volcano (HD-HMMV).

	GD1	GD2	GD3	GD4	GD5	HD-HMMV
GD1	0.3–2.9					
GD2	17.7–20.6	0.3–2.3				
GD3	23.5–25.4	20.6–23.2	0.3–1.9			
GD4	17.4–19.3	21.2–25.7	21.9–25.4	0.3–10.9		
GD5	22.0–23.5	13.3–16.1	22.3–25.7	21.2–25.1	0.3–2.3	
HD-HMMV	19.9–22.0	19.1–20.6	22.7–25.2	22.7–24.1	20.4–22.0	0.3–1.0

length. The *D2D3* alignment contained 29 variable sites, of which 28 were parsimony informative. No insertions and deletions were observed. The average length of the last nuclear fragment (*ITS*) used in the alignment was 800 bp over all sequences. Because of 41 different insertions and deletions, ranging from 1 to 28 bp in length, the total length of the alignment increased to 909 bp. The *ITS* alignment contained 286 variable positions, of which 270 were parsimony informative. When analysing the *ITS* nuclear marker prior to concatenation (Figure S4), GD1 and GD4 (bootstrap values = 100), and GD2 and GD5 (bootstrap values = 100) pooled together as was also observed in the *COI* tree. HD-HMMV now showed a closer relation to the GD1/GD4 clade (bootstrap values: 97, 99, 67, 100 for ML, MP, NJ and BA, respectively), while the position of GD3 remained ambiguous. The *D2D3* sequences of GD1 and GD4, and GD2 and GD5 were identical. Furthermore, HD-HMMV was positioned close to GD1/4 (bootstrap values: 87, 64, 92 and 98 for ML, MP, NJ and BA respectively, Figure S5). The position of the GD3 clade remained unresolved. Even though the position of HD-HMMV and especially of GD3 between the different methods of phylogenetic tree construction remained unresolved, the ILD tests (p = 1) allowed us to combine *ITS* and *D2D3* into a single data set (Supporting information). The concatenated alignment was 1208 bp long with 314 variable sites, of which 297 were parsimony informative. The combined nuclear tree yielded the same topology for all four methods (MP, NJ, ML and BA, Fig. 3A). The MP tree (inferred from five optimal trees) had a tree length of 387. The CI and RI were 0.9121 and 0.9664, respectively. The NJ tree had a length of 389 and a CI and RI of 0.9075 and 0.9644, respectively. Negative ln likelihood values for ML and BA phylogenetic trees were 3498.24 and 3517.67, respectively. The clustering of GD1/GD4 and GD2/GD5 was confirmed with bootstrap values of 100 for both clades in all four analyses. The close relation of HD-HMMV with GD1/GD4 was strengthened and highly supported in most methods (96, 99, 74 and 100 for ML, MP, NJ and BA, respectively). The position of GD3 remained unresolved. Divergences between species ranged between 0.5% and 18.1% (Table 3).

The *18S* phylogenetic trees all showed the same topology. The MP tree (inferred from 17 optimal trees) and NJ tree had a length of 192. The CI = 0.9792 and the RI = 0.9916 were the same for both trees. Negative ln likelihood values for ML and BA phylogenetic trees were 1891.27 and 1918.96, respectively. All methods revealed that the relationships between GD1/4 on the one hand and between GD2/5 clades on the other hand were highly supported (Fig. 3B). Furthermore, HD-HMMV was posi-

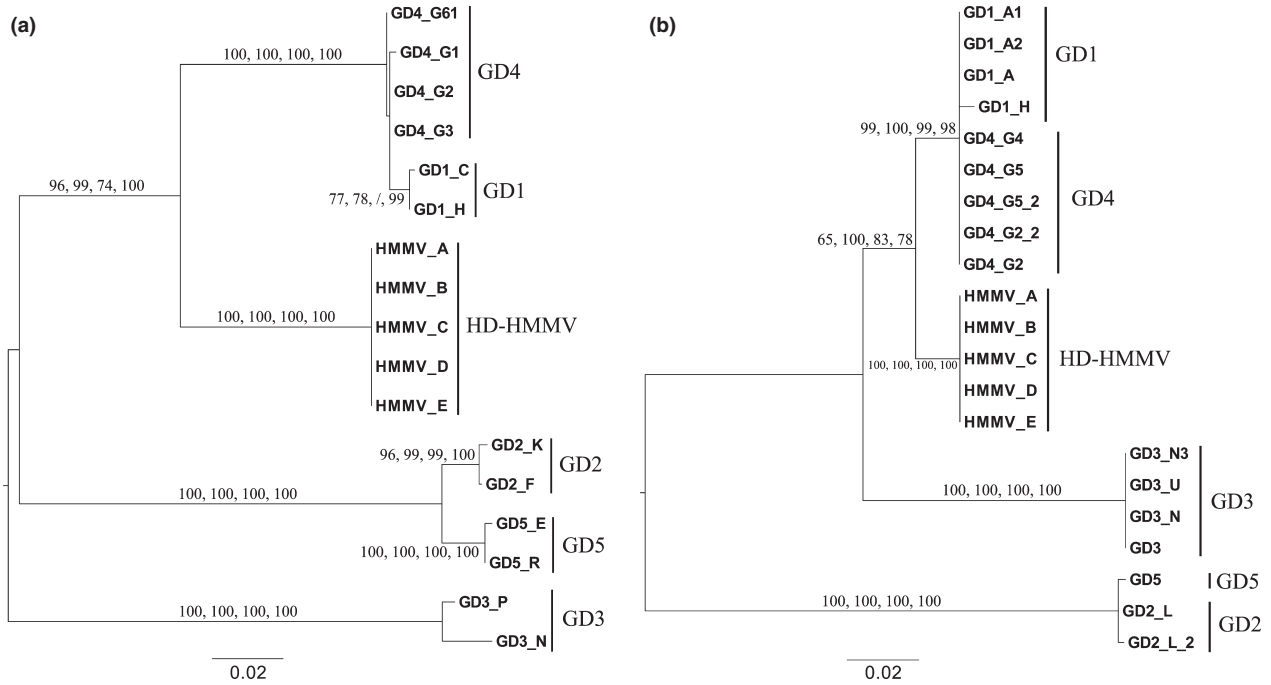

Fig. 3. Maximum likelihood (ML) tree of a heuristic analysis of the concatenated nuclear genes *Internal Transcribed Spacer region* and *D2D3* region of *28S rDNA* (A), and of the *18S rDNA* (B) of shallow-water [*Halomonhystera disjuncta* 1-5 (GD1-5)] and deep-sea (HD-HMMV) nematodes. Bootstrap values above each branch correspond to ML, maximum parsimony, neighbour joining and Bayesian analysis. Trees are mid-point rooted.

Table 3. Interspecific minimum-maximum of uncorrected p-distances (%) between intertidal *Halomonhystera disjuncta* species (GD1-5) and *H. disjuncta* nematodes from the Håkon Mosby mud volcano (HD-HMMV) of the concatenated nuclear genes *Internal Transcribed Spacer region* (*ITS-D2D3*) under the diagonal and *18S* above the diagonal. The diagonal contains the intraspecific minimum-maximum of uncorrected p-distances (%) of both *18S* (*) and *ITS-D2D3* (**).

	GD1	GD2	GD3	GD4	GD5	HD-HMMV
GD1	0.0–0.4* 0.1–0.1**	15.7–16.5	8.7–9.1	0.0–0.4	18.7–19.0	2.4–2.9
GD2	12.9–14.5	0.0–0.2* 0.3–0.3**	18.5–19.6	15.7–16.3	0.2–0.2	16.3–16.8
GD3	12.7–15.0	16.9–17.7	0.0–0.0* 1.6–1.6**	8.7–8.9	22.7–23.2	8.9–9.1
GD4	0.5–0.8	14.4–14.6	13.9–14.8	0.0–0.0* 0.0–0.3**	18.6–18.9	2.4–2.5
GD5	12.7–14.8	2.2–2.4	17.4–18.1	14.7–14.9	0.0–0.0* 0.2–0.2**	19.3–19.3
HD-HMMV	9.5–9.5	14.2–14.3	14.8–15.5	9.3–9.4	14.0–14.0	0.0–0.0* 0.0–0.0**

tioned close to the GD1/4 (65, 100, 83 and 78 for ML, MP, NJ and BA, respectively), but with less support compared to the concatenated tree. The relationships of GD3 with the other clades were again unresolved (Fig. 3B). Divergences between species ranged between 0.0% and 23.2%.

In view of the distinct clade formed by the HMMV specimens in both mitochondrial and nuclear data sets, this clade is treated as a separate species throughout the rest of this work.

Morphometric data

The most pronounced morphological difference between the HD-HMMV and the shallow-water specimens, observed with a light microscope, was the presence of a progaster. The progaster is a narrowing after the first four secretory cells of the intestine (Fig. 4). Scoring absence and presence of this progaster revealed that it is not a unique characteristic. This progaster was exhibited by both HD-HMMV (98%) and shallow-water nematodes (5%). In addition to scoring on absence and presence, we have also measured the progaster diameter (PD) and divided it by the corresponding body diameter (PCBD, Fig. 4). Statistical analysis of the ratio of all six groups revealed a significant difference (ANOVA, $p < 0.05$) between deep-sea and shallow-water nematodes (Fig. 5). These measurements were used in the morphometric analysis that follows.

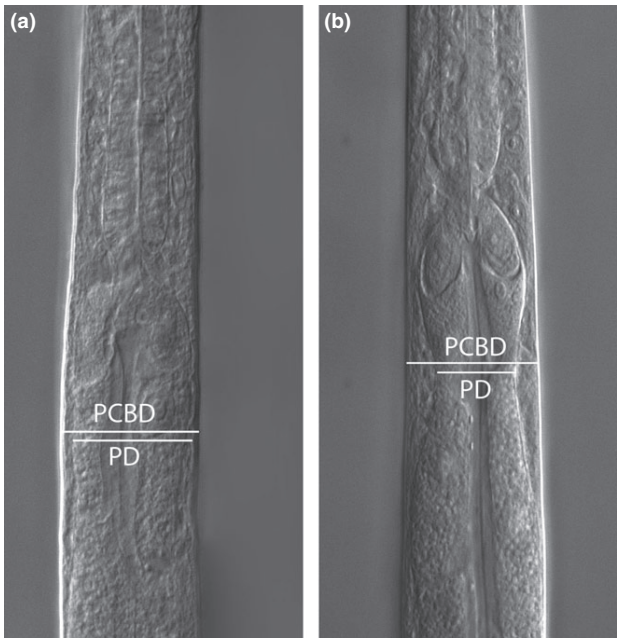

Fig. 4. Microscopic photograph of the progaster in shallow-water (A) and deep-sea nematodes (B). During following analysis, we measured the progaster diameter (PD) and the progaster corresponding body diameter (PCBD) as is shown on the figure above.

The morphometric analysis was carried out on the male and female data set (measurements are summarized in Table S1, all measurements can be found in Table S2 and S3, Supporting information) separately using the six groups observed in the molecular analysis. There was a significant difference in length between the six different nematode species for both females (Kruskal–Wallis $\chi^2 = 23.985$, df = 5, p-value = 0.0002) and males (Kruskal–Wallis $\chi^2 = 30.3274$, df = 5, p-value = 1.27E-05). The HD-HMMV nematodes were significantly smaller compared to all five intertidal species (ANOVA, $p < 0.05$), while pairwise comparisons within the GD1-5 group yielded no significant differences.

The backward stepwise DFA on the female data set revealed that all but two (amphid-anterior distance and TL) of the morphometric characters contributed significantly to the multivariate discrimination between HD-HMMV and GD1-5 (Table 4). Wilks' lambda was 0.01392 and highly significant (ca. $F_{40.543} = 22.267$; $p < 0.0001$). A clear separation of the HD-HMMV-F population and GD1-5-F could be observed along root 1 and accounted for 86.53% of the explained variance (Fig. 6A). The segregation along root 1 was mainly caused by differences in the pharynx length (PL), head diameter (Hdia), PD and PCBD as evidenced by the high correlation of these morphometric characteristics and the canonical root (Table 5). The cross-validation test using the discriminant functions derived from the morphometric features showed that 100% of HD-HMMV-F of the *a priori* grouped cases is classified correctly. For GD1-5-F, these percentages range between 100% (GD3-F) and 41% (GD1-F). Root 2 separates GD1-5-F to a certain extend and reveals a high variance within the HD-HMMV-F population. The differences along root 2 were mostly caused by differences in length between vulva and anus.

The DFA on the male data set also showed a highly significant model (Table 6). Wilks' lambda was 0.02673 and was highly significant (ca. $F_{40.299} = 9.6895$; $p < 0.0001$). Compared to our female DFA, only three morphometric parameters are significant in our model namely PL, amphid-anterior distance (A-A) and the head diameter (Hdia). These three morphometric features capture 96.93% of the variation within the proposed model. It is clear that the HD-HMMV-M population is separated from GD1-

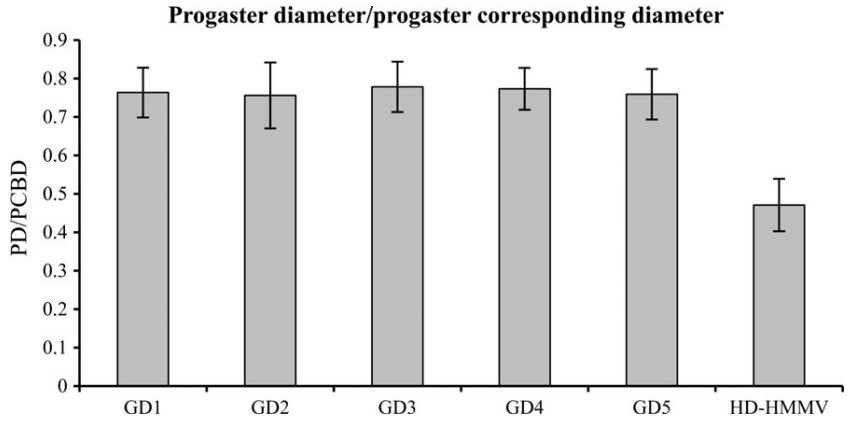

Fig. 5. Plot of the average progaster diameter/corresponding intestine diameter (PD/PCBD) with standard deviations for shallow-water (GD1-5) and deep-sea nematodes (HD-HMMV).

Table 4. Summary of the discriminant function analysis on the morphometric features of female HD-HMMV and female GD1-5. No. of variables in model: 8; 6 groups, Wilks' lambda: 0.01392, ca. $F_{40.543} = 22.267$; $p < 0.0001$.

	Wilks' lambda	Partial lambda	*F*-remove (11.198)	p-level	Toler.	1-Toler.
PL	0.01963	0.70923	10.00345	0.00000	0.69856	0.30144
A-A	0.01501	0.92704	1.92030	0.09572	0.72738	0.27262
Hdia	0.02379	0.58501	17.30882	0.00000	0.72599	0.27401
V-A	0.02278	0.61100	15.53430	0.00000	0.82679	0.17321
ABD	0.01599	0.87045	3.63160	0.00426	0.68217	0.31783
TL	0.01593	0.87367	3.52810	0.00516	0.79860	0.20140
PD	0.02700	0.51559	22.92452	0.00000	0.49399	0.50601
PCBD	0.01884	0.73890	8.62187	0.00000	0.40191	0.59809

PL, pharynx length; A-A, amphid anterior distance; Hdia, head diameter; V-A, distance between vulva and anus (females); ABD, anal body diameter; TL, tail length (starts from the anus up to posterior end of the tail); PD, progaster diameter; PCBD, progaster corresponding diameter.

5-M along root 1 (Fig. 6B). As expected, PL, A-A and Hdia showed the highest correlation with root 1 (Table 5). Very similar to the female DFA, males of the GD1-5 species are separated along root 2, but this distinction is not as obvious. The predicted classification compared to the observed of HD-HMMV-M is 100%, while for GD1-5-M, it ranges between 25% (GD5) and 80.95% (GD3). Even though the observed classification GD1-5-M is not perfect, none of the intertidal nematodes were classified within the HD-HMMV-M group.

Population genetic structure of HMMV specimens

AMOVA did not reveal significant differences between the three locations ($\Phi_{ST} = -0.02659$, $p = 0.93$). Pairwise Φ_{ST} values ranged between -0.02222 and -0.03252, but were all not significantly different from zero (p-values > 0.65). The haplotype network (Fig. 7) shows that haplotypes C (56.67%) and D (25.56%) were the most common and accounted for 82.23% of the observed haplotypes. All haplotypes were present in the South West and South East, but haplotypes A and B were not encountered in the North (Fig. 7).

Discussion

Is HD-HMMV conspecific to shallow-water nematodes?

The extensive application of molecular tools in systematic studies has revealed that the number of described morphospecies tends to be an underestimation of the real biological diversity in marine taxa (Knowlton 1993; Meyer and Paulay 2005; Malay and Paulay 2010). Using sequence information for several genes allowed us to identify six different species within the morphologically described *H. disjuncta*, five of which were previously recognized by Derycke et al. (2007a). The mitochondrial and nuclear data reported in this paper clearly show that HD-HMMV, earlier identified as *H. disjuncta* (Van Gaever et al. 2006; Portnova 2009), forms a distinct phylogenetic clade which is in accordance with previous studies (Van Gaever et al. 2009b). This illustrates that HD-HMMV has a distinct evolutionary trajectory and is a different species according to the phylogenetic species concept (Adams 1998). The genetic divergences observed in the *COI* gene within clades (<2.9%, except for GD4) is in agreement with the proposed threshold level of interspecific divergence (5%) for marine nematodes (Derycke et al. 2010b). Divergences between HD-HMMV and GD1-5 range from 19.1% to 25.2%. These divergences are comparable to those observed between different species (Derycke et al. 2010b).

The morphological data also showed clear differences between HD-HMMV and the five shallow-water species. The DFA using the six molecular clades as groups revealed a clear separation of HD-HMMV from the GD1-5 complex for both males and females. The PL, head diameter (through buccal cavity) and the presence of a progaster explained most of the difference between deep-sea and shallow-water species. Previous studies have suggested that the length of the pharynx could be an adaptation to the diet of nematodes (Roggen 1970, 1973). In addition, the buccal cavity (and also the head diameter) of HD-HMMV is 25–40% larger than that of GD1-5 and is also known to be a good indicator for the diet (Jensen 1987, 1992). *Halomonhystera disjuncta* from the shallow water is a bacterivorous opportunistic species surviving in the presence of a high food diversity (Vran-

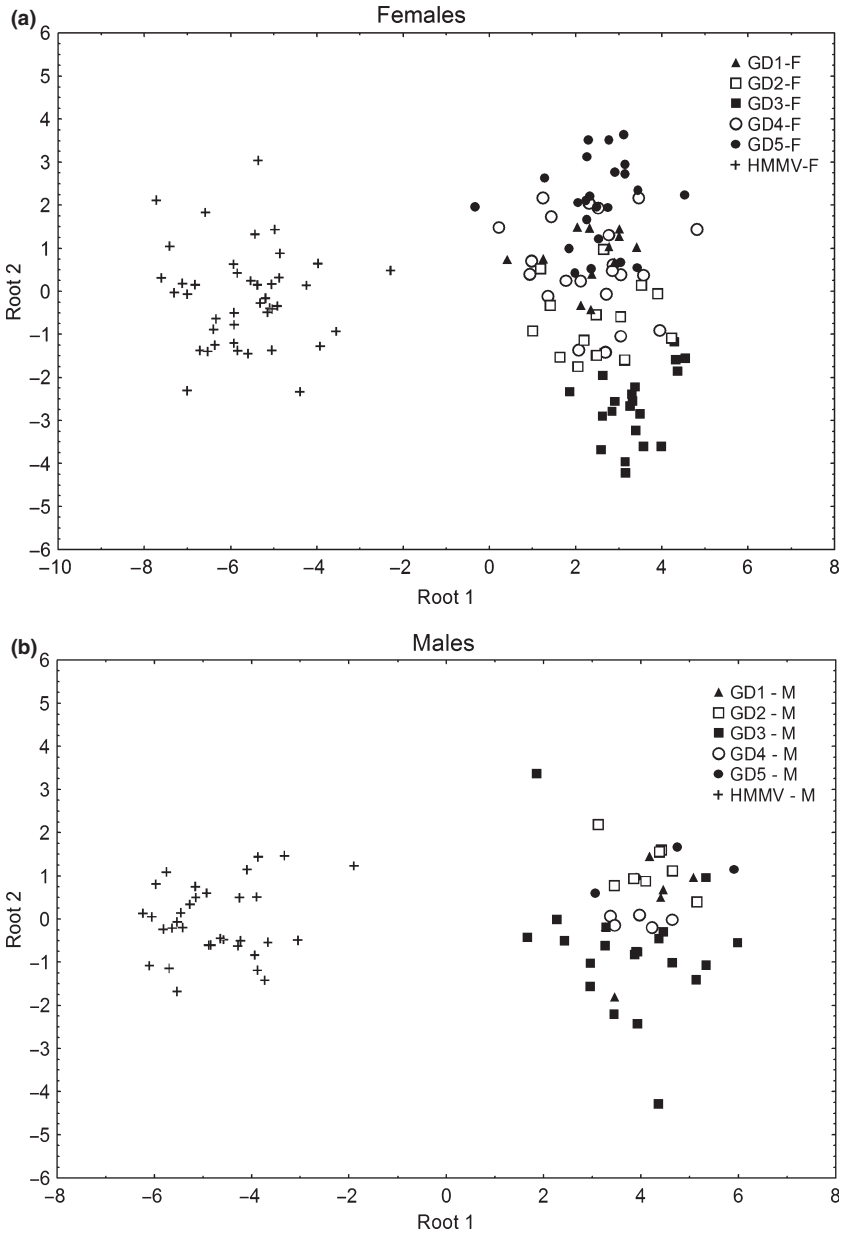

Fig. 6. Canonical scatter plot of the discriminant function analysis scores along the first and second root for the morphometric features of *Halomonhystera disjuncta* which have been mounted in glycerine slides. The deep-sea nematode (HD-HMMV) lineages are represented as a plus sign for both females (A) and males (B).

Table 5. Structure matrix of discriminant loadings for each morphometric variable for root 1 and 2.

	Females		Males	
	Root 1	Root 2	Root 1	Root 2
PL	−11.1064	−9.3934	−12.2058	5.2670
A-A	3.4138	1.2342	8.9834	3.1978
Hdia	−13.0000	6.0534	−17.3690	−3.2824
V-A or SL	3.5563	−15.8004	−1.5043	−1.3382
ABD	2.8719	8.0373	−5.4302	16.7224
TL	−2.3187	−7.5270	−4.3070	−17.0851
PD	16.9927	−0.7826	5.2990	−4.6488
PCBD	−11.5991	10.1090	5.9494	−9.0158

Left = females; right = males; SL, spicule length (other abbreviations as explained in Table 4).

ken et al. 1988a; Moens and Vincx 2000). In contrast, the bacterial mats at HMMV are dominated by *Beggiatoa* (Losekann et al. 2007). The larger buccal cavity of the deep-sea HMMV could be an adaptation to the suggested *Beggiatoa* diet (Van Gaever et al. 2009b), which occur in filaments making it harder to eat and digest. The most anterior midgut cells forming the progaster of *monhysterids* function as secretory cells producing digestive enzymes (Deutsch 1977), which may also aid in the breaking down of these *Beggiatoa* filaments. Even though linking buccal cavity size with diet is tempting, we lack direct observations of feeding behaviour and gut contents, which are necessary to draw firm conclusions of dietary effects on the morphology of HD-HMMV. The progaster has been previously observed in nematodes (Steiner 1958; Chitwood and Murphy 1964), even in deep-sea nematodes (Jensen 1991). Our results

Table 6. Summary of the discriminant function analysis on the morphometric features of male HD-HMMV and male GD1-5. No. of variables in model: 8; 6 groups, Wilks' lambda: 0.02673, ca. $F_{40.299} = 9.6895$; $p < 0.0001$.

	Wilks' lambda	Partial lambda	*F*-remove (11.198)	p-level	Toler.	1-Toler.
PL	0.035454	0.754039	4.43621	0.001481	0.612625	0.387375
A-A	0.033398	0.800462	3.39019	0.008570	0.559192	0.440808
Hdia	0.055218	0.484151	14.49042	0.000000	0.591645	0.408355
SL	0.028155	0.949522	0.72300	0.608482	0.883521	0.116479
ABD	0.030793	0.868192	2.06474	0.080529	0.468351	0.531649
TL	0.030732	0.869900	2.03399	0.084746	0.588614	0.411386
PD	0.028713	0.931071	1.00683	0.420523	0.590864	0.409136
PCBD	0.029582	0.903731	1.44873	0.218234	0.290288	0.709712

Abbreviations as explained in Tables 4–5.

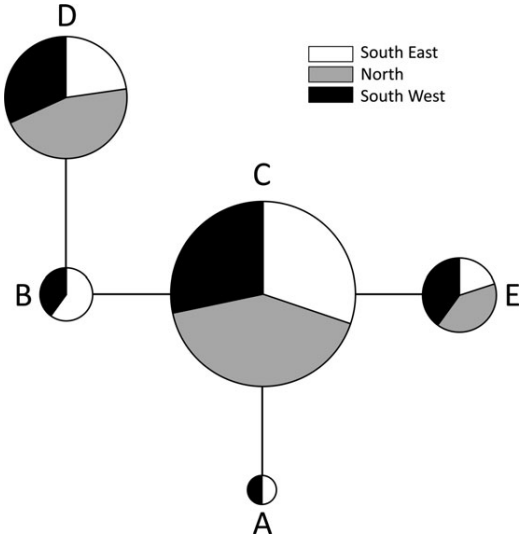

Fig. 7. Minimum spanning network of the thirteen Cytochrome oxidase c subunit I (COI) haplotypes (A–E) of Halomonhystera disjuncta from the South East (white), the North (grey) and the South West (black) of the Håkon mosby mud volcano (HMMV). The surface area of each haplotype corresponds with the frequency of the haplotypes in the total HMMV sample. Branch length has no meaning.

show that the deep-sea habitat favours nematodes with a progaster. This may be caused either by selection or by phenotypic plasticity. Regardless of the evolutionary process leading to the presence of the progaster, it was not exclusively associated with the deep-sea form and is therefore not a diagnostic morphological character to discriminate the deep-sea from the shallow-water form. Furthermore, other morphometric features are significantly different between the deep-sea and intertidal species, indicating that feeding strategy alone cannot be responsible for the observed differences. Whatever the driving force behind the morphological differences may be, our data show that the previously assumed widespread distribution of a single species in quite distinct habitats (deep sea versus intertidal) actually turns out to be a disjunct distribution of cryptic species. A proper taxonomic description of HD-HMMV along with a scientific name is provided by A. Tchesunov, D. Portnova, J. Van Campenhout (in preparation).

Our results further confirm that an integrative approach aids in species discovery and identification of nematodes (De Ley and Blaxter 2002; Holterman et al. 2006; Meldal et al. 2007; Derycke et al. 2010a) and highlights that morphometric features such as the progaster, vulva-anus distance, the anal body diameter and the amphid anterior distance are suitable for discriminating HD-HMMV from their shallow-water relatives.

Phylogenetic relationship between HD-HMMV and the shallow-water species

Our nuclear sequence data further reveal that HD-HMMV is more closely related to GD1/GD4 than to the three remaining cryptic species GD2/GD3/GD5 (Table 3). The evolution of the *rDNA* genes is slower than that of *COI* and is influenced by factors such as functional and structural constraints, unequal crossing over and gene conversion, which all reduce intraspecific variation (Hillis and Dixon 1991). Furthermore, mitochondrial genes have higher mutation rates and a fourfold smaller effective size, so that they consequently evolve more rapidly than nuclear genes (Avise 1995). Saturation of the *COI* gene may therefore blur the deeper phylogenetic relationships. In addition, the length of the *18S* (760 bp) and *ITS-D2D3* concatenated alignment (1208 bp) was much larger than the *COI* alignment used for analysis (343 bp). The differences in evolutionary rate and length of the fragment explain the fact that the relationships between HD-HMMV and its shallow-water relatives are better resolved in the nuclear trees compared to the mitochondrial tree. The topology of the nuclear trees showed that HD-HMMV is an integral part of the shallow-water species complex and suggests an invasion of the deep sea by shallow-water species. If the opposite was true, an invasion of shallow-water habitats from the deep sea, we would expect all five shallow-water species to cluster together with HD-HMMV being the ancestral nematode from which the shallow-water relatives have evolved, which is not the case. A repeated invasion of the deep-sea and shallow-water habitats was also inferred from the tree topology of *Enoplid* marine nematodes (Bik et al. 2010). Similar observations were made for the *Nemertesia* hydroids where the tree topology also showed an interwoven pattern of shallow-water and deep-sea species (Moura et al. 2012).

A successful invasion of deep-sea habitats from shallow waters can be related to the biology of the nematode. *Halomonhystera disjuncta* from intertidal habitats has a higher temperature resistance when compared with brackish water species from the same region (Vranken 1987). In addition, *H. disjuncta* is an early colonizer (Derycke et al. 2007b) and has a large tolerance for heavy metals (Vranken et al. 1988b). Recent experimental data also reveal a tolerance for wide ranges in sulphur concentrations and salinities (J. Van Campenhout, unpublished data). *Halomonhystera disjuncta* is a small nematode (ca. 1 mm) with a short generation time of 1 week and a high reproductive output [ca. 200–500 eggs female^{-1}, (Vranken et al. 1988a)]. As all non-secernentean nematodes, *H. disjuncta* does not produce dauerlarvae, but exhibits a facultative ovoviviparous reproduction strategy (Boffé 1985; Van Gaever et al. 2006), which is an important adaptation allowing nematodes to secure survival and early development of their offspring. This ovoviviparous reproduction strategy has previously been seen as an adaption to changes in environment (Boffé 1985). These features together

with the high food supply at the HMMV could thus have facilitated the successful colonization of the deep sea.

The transfer from shallow water to the deep sea requires dispersal over substantial geographical scales, which is thought to be highly limited for nematodes because they do not have pelagic larvae, and eggs are generally deposited in situ. Phylogeographic and population genetic studies in marine nematodes have revealed that dispersal is substantial at geographical scales of 10–100 km, but highly restricted at larger geographical scales (Derycke et al. 2013). Generally, the lack of a free-swimming life stage or pelagic larval phase limits long-distance dispersal, but given enough offspring and time, some animals will be able to colonize new habitats at long distances from the parental population (Leese et al. 2010). Such infrequent long-distance dispersal has been observed for the rhabditid nematode *L. marina* (Derycke et al. 2008b), which has a short generation time, high reproductive output and strong colonization ability comparable to *H. disjuncta* from the shallow water.

The dispersal of marine animals without a pelagic larval phase has different modes: (1) autonomous drifting, (2) creeping, (3) hopping or intergenerational stepping-stone dispersal (4) hitchhiking and (5) rafting (Reviewed in Winston 2012). The occurrence of HD-HMMV was hypothetically explained by means of rafting on macroalgae after the observation of decaying *Fucus* at the HMMV (Van Gaever et al. 2009b). Moreover, observations were made of nematodes rafting on algae (Thiel and Gutow 2005; Derycke et al. 2008b), indicating long-distance dispersal capacities of nematodes despite the lack of pelagic larvae. The occurrence of *H. disjuncta* on macroalgae makes rafting a likely hypothesis. However, different modes of dispersal remain possible. Because *H. disjuncta* has no dauerlarvae and eggs are generally deposited in situ, autonomous drifting over large distances without any food source seems the most unlikely. Autonomous drifting can be more successful if favourable sedimentary microhabitats are present along its way (hopping). *Halomonhystera disjuncta* is also present at the Nyegga pockmark (64°N 5°E) offshore mid-Norway (Portnova et al. 2010). This pockmark could be a stepping stone for dispersal from shallow water to the HMMV. Unfortunately, we do not have any genetic information for nematodes from this location. In addition, *H. disjuncta* also occurs in marine sediments (Heip et al. 1985; Vranken 1987). Consequently, creeping in the sediment from shallow to the deep-sea waters is plausible. As long as a food source is available, nematodes may also be hitchhikers carried in the ballast water of ships to a new region along a coast or over an ocean. As *H. disjuncta* has a broad geographical distribution in shallow-water areas (along the coast of Belgium and the South Western part of The Netherlands, Western Canada, the White Sea in Northern Russia and the North Sea South of Norway) and we so far only have data from the North Sea area, we cannot infer the area from which the original dispersal has occurred. Nevertheless, the absence of shared haplotypes and the deep phylogenetic divergences between our shallow-water and deep-sea nematodes results in a deep-sea population that is geographically isolated from the studied shallow-water nematodes. The long distances between suitable habitats can form insurmountable barriers [i.e. 'isolation by distance' (Wright 1943)] even in homogeneous habitats such as the abyssal plains (Zardus et al. 2006). Dispersal can also be limited by bathymetrical distances: morphotypes of the echinoderm *Zoroaster fulgens* are reproductively isolated over bathymetrical distances of ca. 1 km (Howell et al. 2004). The bathymetrical difference (ca. 1280 m) and a distance of ca. 2500 km between the intertidal and deep-sea area are therefore likely to have facilitated the separation of the *Halomonhystera* populations between both areas.

Population genetic structure within the Håkon Mosby mud volcano

The HMMV is a small geographical area of ca. 1 km^2. We have sampled three locations within the HMMV, separated by only several hundreds of metres. The high number of shared haplotypes among the three locations and the low number of mutations between haplotypes indicate that there is substantial gene flow between all three areas. The mud volcano can thus be seen as a homogeneous population. Earlier studies have shown that nematodes are able to disperse up to metres (Gingold et al. 2011; Thomas and Lana 2011) and even kilometres (Derycke et al. 2007b). Active dispersal has also been observed in the deep sea (Gallucci et al. 2008; Guilini et al. 2011). Furthermore, the mud volcano itself is a very dynamic environment, with mud flows and local methane bubbling which can force nematodes into the water column and promote dispersal. The North area was colonized by bacterial mats between 2009 and 2010, which has most likely been followed by a recolonization of nematodes from other parts of the mud volcano. This is supported by the lower number of haplotypes and by the absence of unique haplotypes in the North area, a pattern typical of founder effects (Boileau et al. 1992; De Meester et al. 2002).

Conclusion

In this paper, an integrative approach clearly revealed that the deep-sea form of the originally identified *H. disjuncta* is genetically and morphologically distinct from its shallow-water counterparts and should be described as a new species. We supplied morphometric features to discriminate HD-HMMV from the intertidal species. Our nuclear sequence data reveal that HD-HMMV is embedded within the GD1-5 species complex providing proof for a deep-sea invasion by shallow-water nematodes. The large geographic distance and bathymetrical depth between both locations may explain the genetic distance between lineages. However, other dispersal constraints such as currents need to be considered.

Within the HMMV, we did not observe a genetic structure indicating substantial gene flow at this small geographical scale.

Acknowledgements

We gratefully acknowledge chief scientist A. Boetius and project LOOME coordinator D. De Beer for the sampling opportunity during the RV Maria S. Merian campaign MSM 16/2. We thank the captain and the crew of RV 'Maria S. Merian' for their support with work at sea. We thank IFREMER (France), Woods hole oceanographic institution (MA, USA), for mapping the HMMV using the AUV 'Sentry' and the Renard Centre of Marine Geology (Ghent University, Belgium, ROV 'genesis'). Financial support was provided by the EU projects HERMIONE (no. 226354) and ESONET (no. 036851) and by the DFG for the Maria S. Merian cruise MSM 16/2.

References

Adams BJ (1998) Species concepts and the evolutionary paradigm in modern nematology. J Nematol **30**:1–21.

Andrássy I (1981) Revision of the order Monhysterida (Nematoda) inhabiting soil and inland water. Opusc Zool **17/18**:13–47.

Andrássy I (2006) *Halomonhystera*, a new genus distinct from Geomonhystera Andrássy, 1981 (Nematoda: Monhysteridae). Meiofauna Mar **15**:11–24.

Avise JC (1995) Mitochondrial DNA polymorphism and a connection between genetics and demography of relevance to conservation. Conserv Biol **9**:686–690.

Bik HM, Thomas WK, Lunt DH, Lambshead PJ (2010) Low endemism, continued deep-shallow interchanges, and evidence for cosmopolitan distributions in free-living marine nematodes (order Enoplida). BMC Evol Biol **10**:389.

Boffé A (1985) Vergelijkend toxicologisch onderzoek naar sublethale effecten bij de mariene nematode *Monhystera disjuncta* (Bastian 1865). University Ghent, pp 70.

Boileau MG, Hebert PDN, Schwartz SS (1992) Nonequilibrium gene-frequency divergence – persistent founder effects in natural-populations. J Evol Biol **5**:25–39.

Brandt A, Gooday AJ, Brandao SN, Brix S, Brokeland W, Cedhagen T, Choudhury M, Cornelius N, Danis B, De Mesel I, Diaz RJ, Gillan DC, Ebbe B, Howe JA, Janussen D, Kaiser S, Linse K, Malyutina M, Pawlowski J, Raupach M, Vanreusel A (2007) First insights into the biodiversity and biogeography of the Southern Ocean deep sea. Nature **447**:307–311.

Chitwood BG, Murphy DG (1964) Observations on two marine monhysterids – their classification, cultivation, and behaviour. Trans Am Microsc Soc **83**:311–329.

Clement M, Posada D, Crandall KA (2000) TCS: a computer program to estimate gene genealogies. Mol Ecol **9**:1657–1659.

Copley JTP, Flint HC, Ferrero TJ, Van Dover CL (2007) Diversity of melofauna and free-living nematodes in hydrothermal vent mussel beds on the northern and southern East Pacific Rise. J Mar Biol Assoc U.K. **87**:1141–1152.

De Ley P, Blaxter ML (2002) Systematic Position and Phylogeny. The Biology of Nematodes. Taylor and Francis, London, pp 1–30.

De Meester L, Gomez A, Okamura B, Schwenk K (2002) The monopolization hypothesis and the dispersal-gene flow paradox in aquatic organisms. Acta Oecol Int J Ecol **23**:121–135.

Derycke S, Remerie T, Vierstraete A, Backeljau T, Vanfleteren J, Vincx M, Moens T (2005) Mitochondrial DNA variation and cryptic speciation within the free-living marine nematode Pellioditis marina. Mar Ecol Prog Ser **300**:91–103.

Derycke S, Backeljau T, Vlaeminck C, Vierstraete A, Vanfleteren J, Vincx M, Moens T (2007a) Spatiotemporal analysis of population genetic structure in Geomonhystera disjuncta (Nematoda, Monhysteridae) reveals high levels of molecular diversity. Mar Biol **151**:1799–1812.

Derycke S, Van Vynckt R, Vanoverbeke J, Vincx M, Moens T (2007b) Colonization patterns of Nematoda on decomposing algae in the estuarine environment: community assembly and genetic structure of the dominant species Pellioditis marina. Limnol Oceanogr **52**:992–1001.

Derycke S, Fonseca G, Vierstraete A, Vanfleteren J, Vincx M, Moens T (2008a) Disentangling taxonomy within the Rhabditis (Pellioditis) marina (Nematoda, Rhabditidae) species complex using molecular and morhological tools. Zool J Linn Soc **152**:1–15.

Derycke S, Remerie T, Backeljau T, Vierstraete A, Vanfleteren J, Vincx M, Moens T (2008b) Phylogeography of the Rhabditis (Pellioditis) marina species complex: evidence for long-distance dispersal, and for range expansions and restricted gene flow in the northeast Atlantic. Mol Ecol **17**:3306–3322.

Derycke S, De Ley P, De Ley IT, Holovachov O, Rigaux A, Moens T (2010a) Linking DNA sequences to morphology: cryptic diversity and population genetic structure in the marine nematode Thoracostoma trachygaster (Nematoda, Leptosomatidae). Zoolog Scr **39**:276–289.

Derycke S, Vanaverbeke J, Rigaux A, Backeljau T, Moens T (2010b) Exploring the use of cytochrome oxidase *c* subunit 1 (COI) for DNA barcoding of free-living marine nematodes. PLoS ONE **5**:e13716.

Derycke S, Backeljau T, Moens T (2013) Dispersal and gene flow in free-living marine nematodes. Front Zool **10**:????–????.

Deutsch A (1977) Gut structure and digestive physiology of the free-living marine Nematodes, Chromadorina Germanica (Bütschli, 1874) and *Diplolaimella* sp. PhD Thesis, City University of New York.

Excoffier L, Laval G, Schneider S (2005) Arlequin (version 3.0): an integrated software package for population genetics data analysis. Evol Bioinform **1**:47–50.

Fonseca G, Muthumbi AW, Vanreusel A (2007) Species richness of the genus Molgolaimus (Nematoda) from local to ocean scale along continental slopes. Mar Ecol **28**:446–459.

Fonseca G, Derycke S, Moens T (2008) Integrative taxonomy in two free-living nematode species complexes. Biol J Linn Soc **94**:737–753.

Foucher JP, Dupre S, Scalabrin C, Feseker T, Harmegnies F, Nouze H (2010) Changes in seabed morphology, mud temperature and free gas venting at the Hayenkon Mosby mud volcano, offshore northern Norway, over the time period 2003–2006. Geo-Mar Lett **30**:157–167.

Gallucci F, Moens T, Vanreusel A, Fonseca G (2008) Active colonisation of disturbed sediments by deep-sea nematodes: evidence for the patch mosaic model. Mar Ecol Prog Ser **367**:173–183.

Garson GD (2008) Discriminant function analysis. Statnotes: topics in multivariate analysis. Available at: http://www2.chass.ncsu.edu/garson/pa765/statnote.htm.

Gebruk AV, Krylova EM, Lein AY, Vinogradov GM, Anderson E, Pimenov NV, Cherkashev GA, Crane K (2003) Methane seep community of the Håkon Mosby mud volcano (the Norwegian Sea): composition and trophic aspects. Sarsia **88**:394–403.

Gingold R, Ibarra-Obando SE, Rocha-Olivares A (2011) Spatial aggregation patterns of free-living marine nematodes in contrasting sandy beach micro-habitats. J Mar Biol Assoc U.K. **91**:615–622.

Gollner S, Zekely J, Govenar B, Le Bris N, Nemeschkal HL, Fisher CR, Bright M (2007) Tubeworm-associated permanent meiobenthic communities from two chemically different hydrothermal vent sites on the East Pacific Rise. Mar Ecol Prog Ser **337**:39–49.

Guilini K, Soltwedel T, van Oevelen D, Vanreusel A (2011) Deep-sea nematodes actively colonise sediments, irrespective of the presence of a pulse of organic matter: results from an in-situ experiment. PLoS ONE **6**:e18912.

Hasegawa M, Kishino H, Yano T (1985) Dating of the human-ape splitting by a molecular clock of mitochondrial DNA. J Mol Evol **22**:160–174.

Heip C, Vincx M, Vranken G (1985) The ecology of marine nematodes. Oceanogr Mar Biol **23**:399–489.

Hessler RR, Sanders HL (1967) Faunal diversity in deep-sea. Deep-Sea Res **14**:65–78.

Hessler RR, Thistle D (1975) Place of origin of deep-sea isopods. Mar Biol **32**:155–165.

Hillis DM, Dixon MT (1991) Ribosomal DNA: molecular evolution and phylogenetic inference. Q Rev Biol **66**:411–453.

Holterman M, van der Wurff A, van den Elsen S, van Megen H, Bongers T, Holovachov O, Bakker J, Helder J (2006) Phylum-wide analysis of SSU rDNA reveals deep phylogenetic relationships among nematodes and accelerated evolution toward crown Clades. Mol Biol Evol **23**:1792–1800.

Holterman M, Holovachov O, van den Elsen S, van Megen H, Bongers T, Bakker J, Helder J (2008) Small subunit ribosomal DNA-based phylogeny of basal Chromadoria (Nematoda) suggests that transitions from marine to terrestrial habitats (and vice versa) require relatively simple adaptations. Mol Phylogenet Evol **48**:758–763.

Hopper BE (1969) Marine nematodes of Canada. II. Marine nematodes from the Minas Basin – Scots Bay area of the Bay of Fundy, Nova Scotia. Can J Zool **47**:671–690.

Howell KL, Rogers AD, Tyler PA, Billett DSM (2004) Reproductive isolation among morphotypes of the Atlantic seastar species Zoroaster fulgens (Asteroidea: Echinodermata). Mar Biol **144**:977–984.

Jablonski D, Bottjer DJ (1988) Onshore-offshore evolutionary patterns in post-paleozoic echoniderms. In: Burke RD (ed.), Echinoderms Biology, Proceedings of the 6th International Echinoderm Conference, ????, Rotterdam, pp 81–90.

Jensen P (1987) Feeding ecology of free-living aquatic nematodes. Mar Ecol Prog Ser **35**:187–196.

Jensen P (1991) 9 New and less known nematode species from the deep-sea benthos of the Norwegian Sea. Hydrobiologia **222**:57–76.

Jensen P (1992) Predatory nematodes from the deep-sea – description of species from the Norwegian Sea, diversity of feeding types and geographical-distribution. Cah Biol Mar **33**:1–23.

Kieneke A, Arbizu PMM, Fontaneto D (2012) Spatially structured populations with a low level of cryptic diversity in European marine Gastrotricha. Mol Ecol **21**:1239–1254.

Klecka WR (1980) Discriminant Analysis. Sage Publications, London, UK.

Knowlton N (1993) Sibling species in the Sea. Annu Rev Ecol Syst **24**:189–216.

Lambshead PJD (2004) Marine nematode biodiversity. In: Chen ZX, Chen SY, Dickson DW (eds), Nematology: Advances and Perspectives

Vol 1: Nematode Morphology, Physiology and Ecology, CABI Publishing, Wallingford, UK, pp 436–467.
Leese F, Agrawal S, Held C (2010) Long-distance island hopping without dispersal stages: transportation across major zoogeographic barriers in a Southern Ocean isopod. Naturwissenschaften **97**:583–594.
Levin LA, Sibuet M (2012) Understanding continental margin biodiversity: a new imperative. Ann Rev Mar Sci **4**:79–112.
Lichtschlag A, Felden J, Bruchert V, Boetius A, de Beer D (2010) Geochemical processes and chemosynthetic primary production in different thiotrophic mats of the Hakon Mosby Mud Volcano (Barents Sea). Limnol Oceanogr **55**:931–949.
Losekann T, Knittel K, Nadalig T, Fuchs B, Niemann H, Boetius A, Amann R (2007) Diversity and abundance of aerobic and anaerobic methane oxidizers at the Haakon Mosby Mud Volcano, Barents Sea. Appl Environ Microbiol **73**:3348–3362.
Losekann T, Robador A, Niemann H, Knittel K, Boetius A, Dubilier N (2008) Endosymbioses between bacteria and deep-sea siboglinid tubeworms from an Arctic Cold Seep (Haakon Mosby Mud Volcano, Barents Sea). Environ Microbiol **10**:3237–3254.
Malay MC, Paulay G (2010) Peripatric speciation drives diversification and distributional pattern of reef hermit crabs (Decapoda: Diogenidae: Calcinus). Evolution **64**:634–662.
Meldal BH, Debenham NJ, De Ley P, De Ley IT, Vanfleteren JR, Vierstraete AR, Bert W, Borgonie G, Moens T, Tyler PA, Austen MC, Blaxter ML, Rogers AD, Lambshead PJ (2007) An improved molecular phylogeny of the Nematoda with special emphasis on marine taxa. Mol Phylogenet Evol **42**:622–636.
Meyer CP, Paulay G (2005) DNA barcoding: error rates based on comprehensive sampling. PLoS Biol **3**:e422.
Mickevich MF, Farris J (1981) The implications of congruence in Menidia. Syst Zool **30**:351–370.
Moens T, Vincx M (2000) Temperature, salinity and food thresholds in two brackish-water bacterivorous nematode species: assessing niches from food absorption and respiration experiments. J Exp Mar Biol Ecol **243**:137–154.
Mokievsky VO, Filippova KA, Chesunov AV (2005) Nematode fauna associated with detached kelp accumulations in the subtidal zone of the White Sea. Oceanology **45**:689–697.
Moura CJ, Cunha MR, Porteiro FM, Yesson C, Rogers AD (2012) Evolution of Nemertesia hydroids (Cnidaria: Hydrozoa, Plumulariidae) from the shallow and deep waters of the NE Atlantic and western Mediterranean. Zoolog Scr **41**:79–96.
Muthumbi AW, Vanreusel A, Duineveld G, Soetaert K, Vincx M (2004) Nematode community structure along the continental slope off the Kenyan Coast, Western Indian Ocean. Int Rev Hydrobiol **89**:188–205.
Niemann H, Losekann T, de Beer D, Elvert M, Nadalig T, Knittel K, Amann R, Sauter EJ, Schluter M, Klages M, Foucher JP, Boetius A (2006) Novel microbial communities of the Haakon Mosby mud volcano and their role as a methane sink. Nature **443**:854–858.
Nygren A, Eklof J, Pleijel F (2010) Cryptic species of Notophyllum (Polychaeta: Phyllodocidae) in Scandinavian waters. Organ Divers Evol **10**:193–204.
Nylander JAA (2004) MrModeltest v2. Program distributed by the author. Evolutionary Biology Centre, Uppsala University, ????.
Palmer MA (1988) Dispersal of Marine Meiofauna – a review and conceptual-model explaining passive transport and active emergence with implications for recruitment. Mar Ecol Prog Ser **48**:81–91.
Pawlowski J, Bowser SS, Gooday AJ (2007) A note on the genetic similarity between shallow- and deep-water Epistominella vitrea (Foraminifera) in the Antarctic. Deep Sea Res Part II Top Stud Oceanogr **54**:1720–1726.
Pimenov NV, Savvichev AS, Rusanov II, Lein AY, Ivanov MV (2000) Microbiological processes of the carbon and sulfur cycles at cold methane seeps of the North Atlantic. Microbiology **69**:709–720.
Portnova D (2009) Free-living nematodes from the deep-sea Hakon Mosby Mud Volcano, including the description of two new and three known species. Zootaxa **????**:197–213.
Portnova D, Haflidason H, Todt C (2010) Nematode species distribution patterns at the Nyegga pockmarks. 14th International Meiofauna Conference (FourtIMCo). Ghent, Belgium, pp 174.
Posada D, Buckley TR (2004) Model selection and model averaging in phylogenetics: advantages of akaike information criterion and bayesian approaches over likelihood ratio tests. Syst Biol **53**:793–808.
Posada D, Crandall KA (1998) MODELTEST: testing the model of DNA substitution. Bioinformatics **14**:817–818.
Reveillaud J, Remerie T, van Soest R, Erpenbeck D, Cardenas P, Derycke S, Xavier JR, Rigaux A, Vanreusel A (2010) Species boundaries and phylogenetic relationships between Atlanto-Mediterranean shallow-water and deep-sea coral associated Hexadella species (Porifera, Ianthellidae). Mol Phylogenet Evol **56**:104–114.
Roggen DR (1970) Functional aspects of the lower size-limit of nematodes. Nematologica **16**:532–536.
Roggen DR (1973) Functional morphology of the nematode pharynx: 1. Theory of the soft-walled cylindrical pharynx. Nematologica **19**:349–365.
Ronquist F, Teslenko M, van der Mark P, Ayres DL, Darling A, Hohna S, Larget B, Liu L, Suchard MA, Huelsenbeck JP (2012) MrBayes 3.2: efficient Bayesian phylogenetic inference and model choice across a large model space. Syst Biol **61**:539–542.
Sauter EJ, Muyakshin SI, Charlou J-L, Schlüter M, Boetius A, Jerosch K, Damm E, Foucher J-P, Klages M (2006) Methane discharge from a deep-sea submarine mud volcano into the upper water column by gas hydrate-coated methane bubbles. Earth Planet Sci Lett **243**:354–365.
Seinhorst JW (1959) A rapid method for the transfer of nematodes from fixative to anhydrous glycerin. Nematologica **4**:67–69.
Sepkoski JJ (1991) A model of onshore-offshore change in faunal diversity. Paleobiology **17**:58–77.
Steiner G (1958) *Monhystera Cameroni n.* sp. – a nematode commensal of various crustaceans of the Magdalen Island and Bay of Chaleur (Gulf of St. Lawrence). Can J Zool **36**:269–278.
Stekhoven JHS, de Coninck LA, Adam W (1931) The freeliving marine nemas of the Belgian coast. Musée royal d'histoire naturelle de Belgique.
Swofford DL (1998) PAUP*. Phylogenetic Analysis Using Parsimony (*and other methods). Version 4. Sinauer Associates, Sunderland, MA.
Tamura K, Nei M (1993) Estimation of the number of nucleotide substitutions in the control region of mitochondrial-DNA in humans and chimpanzees. Mol Biol Evol **10**:512–526.
Tamura K, Peterson D, Peterson N, Stecher G, Nei M, Kumar S (2011) MEGA5: molecular evolutionary genetics analysis using maximum likelihood, evolutionary distance, and maximum parsimony methods. Mol Biol Evol **28**:2731–2739.
Tavaré S (1986) Some Probabilistic and Statistical Problems in the Analysis of DNA Sequences. American Mathematical Society: Lectures on Mathematics in the Life Sciences. Amer Mathematical Society, ????, pp 57–86.
Taylor MS, Hellberg ME (2005) Marine radiations at small geographic scales: speciation in neotropical reef gobies (Elacatinus). Evolution **59**:374–385.
Thiel M, Gutow L (2005) The ecology of rafting in the marine environment. II. The rafting organisms and community. Oceanogr Mar Biol **43**:279–418.
Thomas MC, Lana PC (2011) A new look into the small-scale dispersal of free-living marine nematodes. Zoologia (Curitiba) **28**:449–456.
Thompson JD, Gibson TJ, Plewniak F, Jeanmougin F, Higgins DG (1997) The CLUSTAL_X windows interface: flexible strategies for multiple sequence alignment aided by quality analysis tools. Nucleic Acids Res **25**:4876–4882.
Trotter D, Webster JM (1983) Distribution and abundance of marine nematodes on the kelp Macrocystis integrifolia. Mar Biol **78**:39–43.
Van Gaever S, Moodley L, de Beer D, Vanreusel A (2006) Meiobenthos at the Arctic Hakon Mosby Mud Volcano, with a parental-caring nematode thriving in sulphide-rich sediments. Mar Ecol Prog Ser **321**:143–155.
Van Gaever S, Moodley L, Pasotti F, Houtekamer M, Middelburg JJ, Danovaro R, Vanreusel A (2009a) Trophic specialisation of metazoan meiofauna at the HAyenkon Mosby Mud Volcano: fatty acid biomarker isotope evidence. Mar Biol **156**:1289–1296.
Van Gaever S, Olu K, Derycke S, Vanreusel A (2009b) Metazoan meiofaunal communities at cold seeps along the Norwegian margin: influence of habitat heterogeneity and evidence for connection with shallow-water habitats. Deep Sea Res I **56**:772–785.

Vanreusel A, Fonseca G, Danovaro R, da Silva MC, Esteves AM, Ferrero T, Gad G, Galtsova V, Gambi C, Genevois VD, Ingels J, Ingole B, Lampadariou N, Merckx B, Miljutin D, Miljutina M, Muthumbi A, Netto S, Portnova D, Radziejewska T, Raes M, Tchesunov A, Vanaverbeke J, Van Gaever S, Venekey V, Bezerra TN, Flint H, Copley J, Pape E, Zeppilli D, Martinez PA, Galeron J (2010) The contribution of deep-sea macrohabitat heterogeneity to global nematode diversity. Mar Ecol **31**:6–20.

Vogt PR, Cherkashev G, Ginsburg G, Ivanov G, Milkov A, Crane K, Sundvor A, Pimenov N, Egorov A (1997) Haakon Mosby Mud Volcano provides unusual example of venting. Eos Trans AGU **78**:549–557.

Vogt PR, Gardner J, Crane K (1999) The Norwegian-Barents-Svalbard (NBS) continental margin: introducing a natural laboratory of mass wasting, hydrates, and ascent of sediment, pore water, and methane. Geo-Mar Lett **19**:2–21.

Vranken G (1987) An autecological study of free-living marine nematodes. Acad Anal **49**:71–97.

Vranken G, Vanderhaeghen R, Heip C (1985) Toxicity of cadmium to free-living marine and brackish water nematodes (Monhystera-Microphthalma, Monhystera-Disjuncta, Pellioditis-Marina). Dis Aquat Organ **1**:49–58.

Vranken G, Herman PMJ, Heip C (1988a) Studies of the life-history and energetics of marine and brackish-water nematodes 1. Demography of *Monhystera-disjuncta* at different temperature and feeding conditions. Oecologia **77**:296–301.

Vranken G, Tire C, Heip C (1988b) The toxicity of paired metal mixtures to the nematode *Monhystera-disjuncta* (Bastian, 1865). Mar Environ Res **26**:161–179.

Vranken G, Tire C, Heip C (1989) Effect of temperature and food on hexavalent chromium toxicity to the marine nematode *Monhystera-disjuncta*. Mar Environ Res **27**:127–136.

Wilson GDF (1998) Historical influences on deep-sea isopod diversity in the Atlantic Ocean. Deep Sea Res Part II Top Stud Oceanogr **45**:279–301.

Winston JE (2012) Dispersal in marine organisms without a pelagic larval phase. Integr Comp Biol **52**:447–457.

Wright S (1943) Isolation by distance. Genetics **28**:114–138.

Zardus JD, Etter RJ, Chase MR, Rex MA, Boyle EE (2006) Bathymetric and geographic population structure in the pan-Atlantic deep-sea bivalve Deminucula atacellana (Schenck, 1939). Mol Ecol **15**:639–651.

Zekely J, Sørensen M, Bright M (2006) Four new nematode species of family Monhysteridae De Man, 1876 from deep-sea hydrothermal vents from East Pacific Rise and Mid-Atlantic Ridge. Meiofauna Mar **15**:25–42.

Supporting Information

Additional Supporting Information may be found in the online version of this article:

Figure S1. Neighbour joining (NJ) of the mitochondrial *Cytochrome oxidase c subunit I* (*COI*) gene of shallow-water [*Halomonhystera disjuncta* 1-5 (GD1-5)] and deep-sea (HD-HMMV) nematodes.

Figure S2. Bayesian analysis (BA) tree of the mitochondrial *Cytochrome oxidase c subunit I* (*COI*) gene of shallow-water [*Halomonhystera disjuncta* 1-5 (GD1-5)] and deep-sea (HD-HMMV) nematodes.

Figure S3. Maximum parsimony tree of a heuristic analysis of the mitochondrial *Cytochrome oxidase c subunit I* (*COI*) gene of shallow-water [*Halomonhystera disjuncta* 1-5 (GD1-5)] and deep-sea (HD-HMMV) nematodes.

Figure S4. Maximum likelihood tree of a heuristic analysis of the nuclear *Internal Transcribed Spacer region* (*ITS*) gene of shallow-water [*Halomonhystera disjuncta* 1-5 (GD1-5)] and deep-sea (HD-HMMV) nematodes.

Figure S5. Maximum likelihood tree of a heuristic analysis of the nuclear *D2D3* region of *28S rDNA* (*D2D3*) gene of shallow-water [*Halomonhystera disjuncta* 1-5 (GD1-5)] and deep-sea (HD-HMMV) nematodes.

Table S1. Minimum-maximum (μm) and mean (μm) ± standard deviation (between brackets) values of 12 morphological measures from the five shallow-water *Halomonhystera disjuncta* cryptic species GD1-5 and the deep-sea nematode HD-HMMV for both females and males.

Table S2. Morphometric data of 43 female HD-HMMV individuals in μm.

Table S3. Morphometric data of 37 male HD-HMMV individuals in μm.

Data S1. Alignment_COI.fas, Alignment_D2D3-ITS.fas, Alignment_18S.fas.